J|A|C|S
ARTICLES
Published on Web 02/24/2007

Hydration Dynamics and Time Scales of Coupled Water−Protein Fluctuations

Tanping Li,[†] Ali A. Hassanali,[†] Ya-Ting Kao,[§] Dongping Zhong,*[,†,‡,§] and Sherwin J. Singer*[,†,§]

Contribution from the Biophysics Program, and Departments of Physics and Chemistry, The Ohio State University, Columbus, Ohio 43210

Received November 30, 2006; E-mail: dongping@mps.ohio-state.edu; singer@chemistry.ohio-state.edu

Abstract: We report experimental and theoretical studies on water and protein dynamics following photoexcitation of apomyoglobin. Using site-directed mutation and with femtosecond resolution, we experimentally observed relaxation dynamics with a biphasic distribution of time scales, 5 and 87 ps, around the site Trp7. Theoretical studies using both linear response and direct nonequilibrium molecular dynamics (MD) calculations reproduced the biphasic behavior. Further constrained MD simulations with either frozen protein or frozen water revealed the molecular mechanism of slow hydration processes and elucidated the role of protein fluctuations. Observation of slow water dynamics in MD simulations requires protein flexibility, regardless of whether the slow Stokes shift component results from the water or protein contribution. The initial dynamics in a few picoseconds represents fast local motions such as reorientations and translations of hydrating water molecules, followed by slow relaxation involving strongly coupled water−protein motions. We observed a transition from one isomeric protein configuration to another after 10 ns during our 30 ns ground-state simulation. For one isomer, the surface hydration energy dominates the slow component of the total relaxation energy. For the other isomer, the slow component is dominated by protein interactions with the chromophore. In both cases, coupled water−protein motion is shown to be necessary for observation of the slow dynamics. Such biologically important water−protein motions occur on tens of picoseconds. One significant discrepancy exists between theory and experiment, the large inertial relaxation predicted by simulations but clearly absent in experiment. Further improvements required in the theoretical model are discussed.

Introduction

Protein surface hydration is fundamental to its structure, stability, dynamics, and function.[1−14] Femtosecond (fs)-resolved studies of solvation on a series of protein surfaces,[15−22] using intrinsic tryptophan (Trp) as a local optical probe,[15,23−27] have revealed relaxation dynamics on the picosecond (ps) time scales with a biphasic distribution. By observing the fs-resolved fluorescence Stokes shift of the probe upon excitation, the initial dynamics was observed to occur in a few picoseconds and is attributed to fast librational/rotational motions of local water molecules. The second slow relaxation takes tens of picoseconds and was assigned to rearrangements of neighboring water networks around the excited probe,[20−22] although this assignment has been challenged.[28] Relaxation processes on even longer time scales have been observed using other biophysical methods such as dielectric relaxation,[29] neutron scattering,[30] and earlier NMR studies.[11,31]

[†] Biophysics Program.
[‡] Department of Physics.
[§] Department of Chemistry.

(1) Levy, V.; Onuchic, J. N. *Annu. Rev. Biophys. Biomol. Struct.* **2006**, *35*, 389.
(2) Raschke, T. M. *Curr. Opin. Struct. Biol.* **2006**, *16*, 152.
(3) Pal, S. K.; Zewail, A. H. *Chem. Rev.* **2004**, *104*, 2099.
(4) Daniel, R. M.; Finney, J. L.; Stoneham, M. *Philos. Trans. R. Soc. London, Ser. B* **2004**, *359*, 1143.
(5) Wüthrich, K. *Angew. Chem., Int. Ed.* **2003**, *42*, 3340.
(6) Mattos, C. *Trends Biochem. Sci.* **2002**, *27*, 203.
(7) Gregory, R. B., Ed. *Protein-Solvent Interaction*; Marcel Dekker: New York, 1995.
(8) Bryant, R. G. *Annu. Rev. Biophys. Biomol. Struct.* **1996**, *25*, 29.
(9) Timasheff, S. N. *Annu. Rev. Biophys. Biomol. Struct.* **1993**, *22*, 67.
(10) Teeter, M. M. *Annu. Rev. Biophys. Biophys. Chem.* **1991**, *20*, 577.
(11) Otting, G.; Liepinsh, E.; Wüthrich, K. *Science* **1991**, *254*, 974.
(12) Levitt, M.; Sharon, R. *Proc. Natl. Acad. Sci. U.S.A.* **1988**, *85*, 7557.
(13) Bizzarri, A. R.; Cannistraro, S. *J. Phys. Chem. B* **2002**, *106*, 6617.
(14) Bagchi, B. *Chem. Rev.* **2005**, *105*, 3197.
(15) Zhong, D.; Pal, S. K.; Zhang, D.; Chan, S. I.; Zewail, A. H. *Proc. Natl. Acad. Sci. U.S.A.* **2002**, *99*, 13.
(16) Pal, S. K.; Peon, J.; Zewail, A. H. *Proc. Natl. Acad. Sci. U.S.A.* **2002**, *99*, 1763.
(17) Peon, J.; Pal, S. K.; Zewail, A. H. *Proc. Natl. Acad. Sci. U.S.A.* **2002**, *99*, 10964.
(18) Zhao, L.; Pal, S. K.; Xia, T.; Zewail, A. H. *Angew. Chem., Int. Ed.* **2004**, *43*, 60.
(19) Pal, S. K.; Peon, J.; Bagchi, B.; Zewail, A. H. *J. Phys. Chem. B* **2002**, *106*, 12376.
(20) Qiu, W.; Zhang, L.; Kao, Y. T.; Lu, W.; Li, T.; Kim, J.; Sollenberger, G. M.; Wang, L.; Zhong, D. *J. Phys. Chem. B* **2005**, *109*, 16901.
(21) Qiu, W.; Zhang, L.; Okobiah, O.; Yang, Y.; Wang, L.; Zhong, D.; Zewail, A. H. *J. Phys. Chem. B* **2006**, *110*, 10540.
(22) Qiu, W.; Kao, Y. T.; Zhang, L.; Wang, L.; Stites, W. E.; Zhong, D.; Zewail, A. H. *Proc. Natl. Acad. Sci. U.S.A.* **2006**, *103*, 13979.
(23) Shen, X.; Knutson, J. R. *J. Phys. Chem. B* **2001**, *105*, 6260.
(24) Lu, W.; Kim, J.; Qiu, W.; Zhong, D. *Chem. Phys. Lett.* **2004**, *388*, 120.
(25) Lu, W.; Qiu, W.; Kim, J.; Okobiah, O.; Hu, H.; Gokel, G. W.; Zhong, D. *Chem. Phys. Lett.* **2004**, *394*, 415.
(26) Zhang, L.; Kao, Y. T.; Qiu, W.; Wang, L.; Zhong, D. *J. Phys. Chem. B* **2006**, *110*, 18097.
(27) Kim, J.; Lu, W.; Qiu, W.; Wang, L.; Caffrey, M.; Zhong, D. *J. Phys. Chem. B* **2006**, *110*, 21994.
(28) Nilsson, L.; Halle, B. *Proc. Natl. Acad. Sci. U.S.A.* **2005**, *102*, 13867.

10.1021/ja0685957 CCC: $37.00

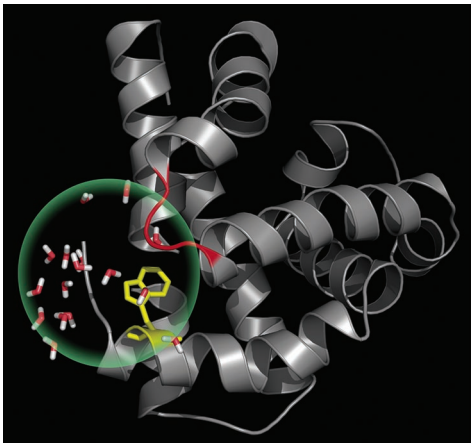

Figure 1. The X-ray structure of *Sperm-Whale* myoglobin (PDB: 1MBD) with 1.7 Å resolution.[32] Also shown is the local site of the optical probe Trp7 with the neighboring flexible loop (79−82) and hydrating water molecules within 7 Å from indole.

In this Article, we report experimental and theoretical studies on water and protein dynamics of *Sperm-Whale* myoglobin (Mb) following photoexcitation of a particular site, Trp7. Figure 1 shows the X-ray structure of the protein, consisting of eight α-helices with a total of 154 amino acids.[32] The wild-type Mb contains two intrinsic tryptophans, Trp7 and Trp14. Experimentally, we mutated Trp14 into tyrosine and measured the total Stokes shift, solvation dynamics, and local rigidity of the single Trp7 with femtosecond resolution. Theoretically, we examined the relaxation dynamics around Trp7 using both linear-response theory and direct nonequilibrium molecular dynamics (MD) simulations following initial photoexcitation. Understanding the origin of the second slow component is the focus of our simulation studies. To deepen the analysis of these slow relaxation processes, we performed additional MD simulations in which protein motion is frozen to isolate and quantify the inherent relaxation dynamics of hydrating water molecules near the protein surface. Alternatively, we constrained water motions to establish the role of solvent dynamics in driving protein fluctuations. These studies reveal the molecular origin of slow hydration dynamics, role of protein fluctuations, and time scales of water−protein interactions. Finally, we present a unified molecular mechanism of protein surface hydration for Trp7 in myoglobin that appears applicable to many other proteins recently studied.[15−22]

Methods

Experimental Methods. The protein mutant W14Y was made possible by a generous gift of plasmid pMb122 (Prof. Stephen Sligar, UIUC). The mutant protein was expressed in *E. coli* and purified mainly following the previous procedures.[33] To avoid energy-transfer quenching between the excited Trp7 and the heme group,[34] we removed the heme[35] and used apo-Mb for solvation studies. The local structures around Trp7 in apo- and holo-Mb are similar.[36,37] The protein was dissolved in the buffer of 10 mM sodium acetate at pH 6.1, and its concentration used in fs-resolved studies was 200−300 μM. To ensure that no change of the protein quality during data acquisition has occurred, we measured the protein fluorescence emission before and after experiments. We also kept the sample in a rotating cell to minimize possible photobleaching.

All measurements of transients were carried out using the fs-resolved fluorescence up-conversion apparatus described before.[26,38] Briefly, the pump laser was set at 290 nm, and its energy was typically attenuated to ∼140 nJ prior to being focused into the motor-controlled moving sample cell. The fluorescence emission was collected by a pair of parabolic mirrors and mixed with a gating pulse (800 nm) in a 0.2-mm BBO crystal through a noncollinear configuration. The up-converted signal ranging from 218 to 292 nm was detected. The instrument response time under the current noncollinear geometry is between 400 and 500 fs as determined from the up-conversion signal of Raman scattering by water at around 320 nm. All measurements were performed at the magic-angle (54.7°) condition.

Simulation Methods. Simulations for the protein were conducted using a double precision version of the GROMACS package[39] and GROMOS96 force field.[40] We used the SPC/E water model because dynamical properties like the diffusion constant are in good agreement with experiment. Also, van Gunsteren and co-workers obtained better agreement with experimental reorientation times for the tryptophan monopeptide using GROMOS96 and SPC/E water.[41] In a study of the hydration dynamics of the Lys−Trp−Lys tripeptide, we found that the SPC and SPC/E water models gave similar hydration energies.[42] The nonbonded pair list was produced using a 9 Å cutoff. Long-range electrostatic interactions were handled using the smoothed particle mesh Ewald (SPME) algorithm[43,44] with a real space cutoff length of 9 Å. The cutoff length for the Lennard-Jones potential was set at 14 Å. All bond lengths were constrained using the LINCS algorithm,[45] allowing a 2 fs time step in the simulation. Periodic boundary conditions were implemented using a truncated triclinic box of side length 60 Å and solvated with 4537 water molecules. The Nose−Hoover thermostat[46−48] was used to maintain the system at 295 K. The initial configuration of myoglobin is taken from the crystal structure (PDB: 1MBD).

Site charges of the indole chromophore in the S_0 state came from the GROMOS96 force field. For the L_a excited state of the indole ring, which is the fluorescing state of Trp in the protein, we modified the partial charge of the indole chromophore by applying the ab initio charge density differences calculated by Sobolewski and Domcke[49] to the ground-state partial charges of the GROMOS96 force field as described in ref 42. At each configuration of the system, the energy difference between the L_a and S_0 state associated with portion x of the system (x = protein, water, total) is denoted by $\Delta E^x(t)$, which in our simplified model is the Coulomb interaction difference between the system with excited- and ground-state charges on the indole of W7, as well as a gas-phase transition energy that is irrelevant for the calculated Stokes shift. The nonequilibrium Stokes shift is the average $\langle \Delta E^x(t) - \Delta E^x(0) \rangle$ over trajectories that evolve on the L_a state surface with initial conditions sampled from an equilibrium ensemble on the S_0 surface. The linear response approximation to the Stokes shift from component

(29) Grant, E. H. *Bioelectromagnetics* **1982**, *3*, 17.
(30) Cheng, X. D.; Schoenborn, B. P. *J. Mol. Biol.* **1991**, *220*, 381.
(31) Otting, G. *Prog. Nucl. Magn. Reson. Spectrosc.* **1997**, *31*, 259.
(32) Phillips, S. E.; Schoenborn, B. P. *Nature* **1981**, *292*, 81.
(33) Springer, B. A.; Sligar, S. G. *Proc. Natl. Acad. Sci. U.S.A.* **1987**, *84*, 8961.
(34) Hochstrasser, R. M.; Negus, D. K. *Proc. Natl. Acad. Sci. U.S.A.* **1984**, *81*, 4399.
(35) Teale, F. W. J. *Biochim. Biophys. Acta* **1959**, *35*, 543.
(36) Lecomte, J. T.; Kao, Y. H.; Cocco, M. J. *Proteins* **1996**, *25*, 267.
(37) Elieze, D.; Wright, P. E. *J. Mol. Biol.* **1996**, *263*, 531.
(38) Saxena, C.; Sancar, A.; Zhong, D. *J. Phys. Chem. B* **2004**, *108*, 18026.
(39) Lindahl, E.; Hess, B.; van der Spoel, D. *J. Mol. Model* **2001**, *7*, 306.
(40) van Gunsteren, W. F.; Billeter, S. R.; Eising, A. A.; Hünenberger, P. H.; Krüger, P.; Mark, A. E.; Scott, W. R. P.; Tironi, I. G. *Biomolecular simulation: The gromos96 manual and user guide*; 1996.
(41) Daura, X.; Suter, R.; van Gunsteren, W. F. *J. Chem. Phys.* **1999**, *110*, 3049.
(42) Hassanali, A. A.; Li, T.; Zhong, D.; Singer, S. *J. Phys. Chem. B* **2006**, *110*, 10497.
(43) Darden, T.; York, D.; Pedersen, L. *J. Chem. Phys.* **1993**, *98*, 10089.
(44) Perera, U. E. L.; Berkowitz, M. L.; Darden, T.; Lee, H.; Pedersen, L. G. *J. Chem. Phys.* **1995**, *103*, 8577.
(45) Hess, B.; Bekker, H.; Berendsen, H. J. C.; Fraaije, J. G. E. M. *J. Comput. Chem.* **1997**, *18*, 1463.
(46) Nosè, S. *Mol. Phys.* **1984**, *52*, 255.
(47) Nosè, S. *J. Chem. Phys.* **1984**, *81*, 511.
(48) Hoover, W. G. *Phys. Rev. A* **1985**, *31*, 1695.
(49) Sobolewski, A. L.; Domcke, W. *Chem. Phys. Lett.* **1999**, *315*, 293.

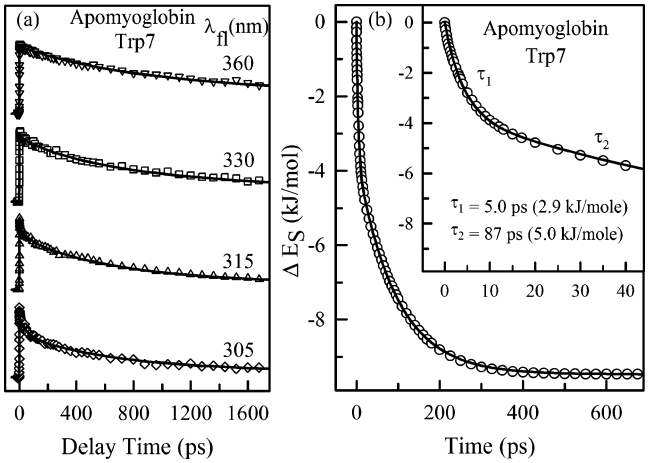

Figure 2. Experimentally measured solvation dynamics. (a) Normalized, femtosecond-resolved fluorescence transients of Trp7 with a series of gated fluorescence emissions from the blue to red side. (b) The derived total Stokes shift changes with time, representing a time-resolved correlation function of local relaxation. The inset shows the dynamics in the short-time range.

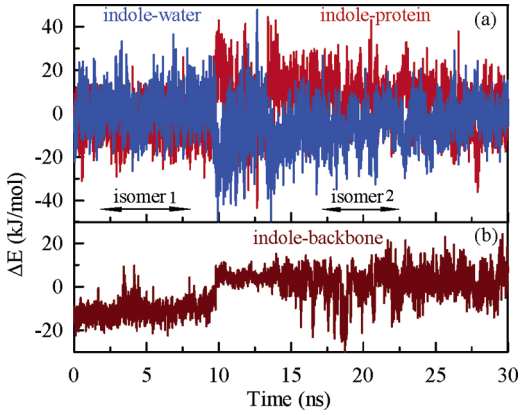

Figure 3. Time evolution of the energy differences between the excited and ground states for the indole (Trp7) with the protein and water in (a), and with the backbone of the loop (residues 79−86) in (b). A structural transition occurs at about 10 ns, and two structures, defined as isomer 1 and isomer 2, were used to perform MD simulations, respectively.

x of the system is given by $1/k_BT[\langle \Delta E^x(t)\Delta E(0)\rangle - \langle \Delta E^x(0)\Delta E(0)\rangle]$,[28] where k_B is Boltzmann's constant and T is the temperature.

Results and Discussion

Femtosecond-Resolved Transients and Local Relaxation Dynamics. The steady-state fluorescence emission of Trp7 in the mutant apoMb (Trp14Tyr) gives a maximum at 332.6 nm. Figure 2a shows the fs-resolved fluorescence transients of several typical wavelengths, from the blue to red side, for more than 10 gated emissions. The overall decay dynamics is significantly slower than that of aqueous tryptophan in a similar buffer solution.[24] Clearly, the ultrafast decay components (<1 ps) observed in tryptophan solution were not observed at the blue side for the protein. Besides the lifetime contributions, all blue-side transients are well represented by a double-exponential decay with time constants ranging from 1.2 to 7.9 ps and from 50 to 102 ps. For the red-side emission, the initial rise occurs in the range of 0.5−1 ps.

Using the methodology we recently developed,[24] we constructed the overall and lifetime-associated fs-resolved emission spectra.[20,21] By fitting these spectra to a lognormal function, we deduced the fs-resolved overall emission maxima (ν_s) and lifetime-associated emission maxima (ν_l). The total dynamic Stokes shift equals $\nu_s - \nu_l$ at time zero, giving ~660 cm^{-1} (7.9 kJ/mol) for Trp7. The possible contribution of vibrational relaxation[20] is negligible, and thus the observed total Stokes shift is from local environment relaxation. Taking the time-zero emission peak as a reference and using $\Delta\nu_{Stokes}(t) = [\nu_s(t) - \nu_l(t)] - [\nu_s(0) - \nu_l(0)]$, we constructed the total relaxation dynamics, and the obtained result is shown in Figure 2b. Similar to many proteins studied in this laboratory[20−22] and Zewail's group,[16−18] the dynamics can be represented by a double-exponential decay. The first component has a time constant of 5 ps and contributes 2.9 kJ/mol to the overall Stokes shift, and the corresponding values for the second component are 87 ps and 5.0 kJ/mol. No ultrafast relaxation dynamics in less than 1 ps was observed for this protein.

Linear-Response Correlation Function versus Direct Non-equilibrium Response. Myoglobin has been studied extensively using MD simulations.[50−64] Most of these studies involve trajectories of much less than 1 nanosecond (ns) except a few simulations of length 0.7−1.1,[57] 1−2,[58] 1,[61] 80,[62] and 90 ns.[63] We sampled a trajectory of ground-state myoglobin extending over 30 ns after initial equilibration for 800 ps and found structural fluctuations occurring on time scales extending up to several nanoseconds. Figure 3a, a plot of the energy differences between the excited and ground states, shows sudden changes (20 kJ/mol) of the indole−water and indole−protein interaction energies after 10 ns occurring in a complementary way, indicating a structural transition. Further examination of the structures before and after 10 ns revealed that the loop backbone between helices E and F with residues 77−86 underwent significant displacement. Most of the resulting energy change is contained in the interaction between loop backbone and chromophore, as shown in Figure 3b. The loop is closer to the indole during the first 10 ns. After the transition, the loop residues fluctuate more, and the helix F is more disordered near the loop. We refer to the structure of the first 10 ns of the trajectory as isomer 1, and the remainder of the trajectory as isomer 2 (Figure 3a). This transition between isomer 1 and isomer 2 is probably a dynamic hopping between local substates.[65−68]

(50) Levy, R. M.; Sheridan, R. P.; Keepers, J. W.; Dubey, G. S.; Swaminathan, S.; Karplus, M. *Biophys. J.* **1985**, *48*, 509.
(51) Henry, E. R.; Eaton, W. A.; Hochstrasser, R. M. *Proc. Natl. Acad. Sci. U.S.A.* **1986**, *83*, 8982.
(52) Elber, R.; Karplus, M. *Science* **1987**, *235*, 318.
(53) Brooks, C. L., III. *J. Mol. Biol.* **1992**, *227*, 375.
(54) Steinbach, P. J.; Brooks, B. R. *Proc. Natl. Acad. Sci. U.S.A.* **1993**, *90*, 9135.
(55) Furois-Corbin, S.; Smith, J. C.; Kneller, G. R. *Proteins* **1993**, *16*, 141.
(56) Clarage, J. B.; Romo, T.; Andrews, B. K.; Pettitt, B. M.; Phillips, G. N. *Proc. Natl. Acad. Sci. U.S.A.* **1995**, *92*, 3288.
(57) Hirst, J. D.; Brooks, C. L., III. *Biochemistry* **1995**, *34*, 7614.
(58) Simonson, T.; Brooks, C. L., III. *J. Am. Chem. Soc.* **1996**, *118*, 8452.
(59) Rovira, C.; Parrinello, M. *Int. J. Quantum Chem.* **2000**, *80*, 1172.
(60) Makarov, V. A.; Andrews, B. K.; Smith, P. E.; Pettitt, B. M. *Biophys. J.* **2000**, *79*, 2966.
(61) Tournier, A. L.; Smith, J. C. *Phys. Rev. Lett.* **2003**, *91*, 208106.
(62) Aschi, M.; Zazza, C.; Spezia, R.; Bossa, C.; Di Nola, A.; Paci, M.; Amadei, A. *J. Comput. Chem.* **2004**, *25*, 974.
(63) Bossa, C.; Anselmi, M.; Roccatano, D.; Amadei, A.; Vallone, B.; Brunori, M.; Di Nola, A. *Biophys. J.* **2004**, *86*, 3855.
(64) Gu, W.; Schoenborn, B. P. *Proteins* **1995**, *22*, 20.
(65) Frauenfelder, H.; Parak, F.; Young, R. D. *Annu. Rev. Biophys. Biophys. Chem.* **1988**, *17*, 451.
(66) Frauenfelder, H.; et al. *J. Phys. Chem.* **1990**, *94*, 1024.
(67) Frauenfelder, H.; Sligar, S. G.; Wolynes, P. G. *Science* **1991**, *254*, 1589.

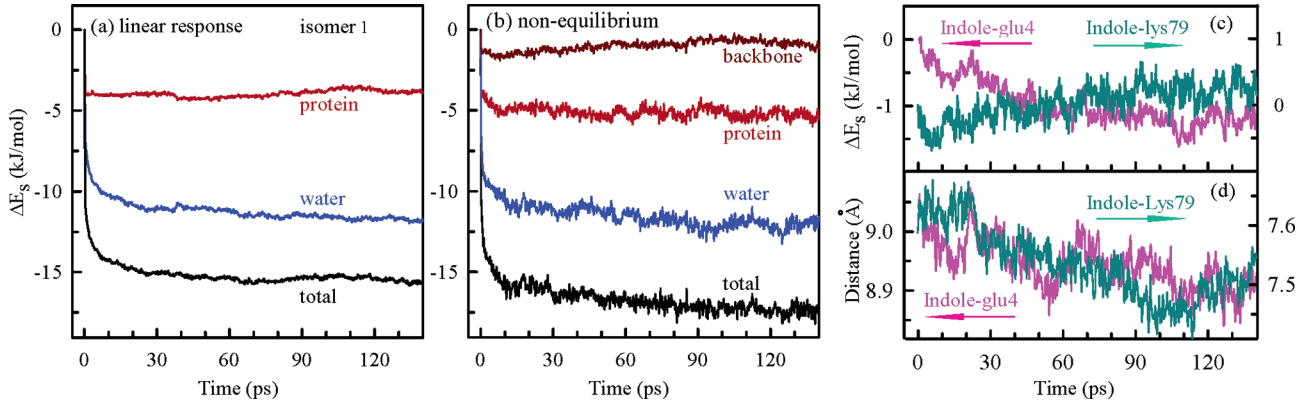

Figure 4. Solvation dynamics from MD simulations for isomer 1. (a) The linear-response calculated time-resolved Stokes shifts for indole−protein, indole−water, and their sum. The indole−water shows an apparent slow component, but the indole−protein exhibits no contribution in the long-time range. (b) Direct nonequilibrium simulations of the time-resolved Stokes shifts for indole−water, indole−protein, and their sum. Similar to (a), the indole−water relaxation has a slow decay component, and the indole−protein lacks long-time decay behavior. Also shown is the indole−backbone interaction, whose magnitude diminishes at long times, complementary to the increase in water response. (c) Relaxation of two neighboring charged residues of a salt bridge, indole−lys79 and indole−glu4. The interaction energy changes from these two residues cancel each other. (d) The distance changes between the indole and two charged residues, which both move closer to the indole ring after photoexcitation.

The relaxation dynamics (Figure 2b) is the response of the environment around Trp7 to its sudden shift in charge distribution from the ground state to the excited state. Under this perturbation, the response can result from both the surrounding water molecules and the protein. We separately calculated the linear-response correlation functions of indole−water, indole−protein,[28] and the sum of the two. The results for isomer 1, relative to the time-zero values, are shown in Figure 4a. The linear response correlation function is accumulated from a 6 ns interval indicated in Figure 3a during which the protein was clearly in the isomer 1 substate. All three correlation functions show a significant ultrafast component: 63% for the total response, 50% for indole−water, and nearly 100% for indole−protein. A fit to the total correlation function beyond the ultrafast inertial decrease requires two exponential decays: 1.4 ps (3.6 kJ/mol) and 23 ps (2.0 kJ/mol). Despite the 6 ns simulation window for isomer 1, the 23 ps long component is not well determined on account of the noise apparent in the linear response correlation function (Figure 4a) between 30 and 140 ps. The slow dynamics are mainly observed in the indole−water relaxation, and the overall indole−protein interactions apparently make nearly no contribution to the slowest relaxation component.

We also performed direct nonequilibrium simulations following photoexcitation. The initial configurations were sampled from the same time interval used to generate the linear-response correlation function (Figure 3a). The results are shown in Figure 4b for isomer 1 with the average of 360 trajectories. The nonequilibrium results up to 140 ps are similar to those from linear-response calculations in Figure 4a. Indole−water interactions make the dominant contributions to the slow component of the total response, and the indole−protein contribution is minor after ~10 ps. The total relaxation dynamics can be fitted by an 18-fs inertial component (4.0 kJ/mol) and three exponentials: 0.080 ps (6.1 kJ/mol), 1.6 ps (4.9 kJ/mol), and 56 ps (2.7 kJ/mol), and the total Stokes shift is 17.7 kJ/mol (15.5 kJ/mol for linear response). Because the loop is flexible near the indole, we examined the indole−backbone interaction and found a rise in energy with time (Figure 4b), coupled to a complementary decrease in the interaction with water. We further studied the two neighboring charged residues of a salt bridge, glu4 and lys79. We found both residues moved close to the indole ring (Figure 4d), but the interaction energies nearly cancel each other (Figure 4c), making no apparent contribution to the indole−protein stabilization. The data in Figure 4 clearly indicate that the water contribution dominates the long-time Stokes shift, yet both the neighboring water and protein rearrange their local configurations following photoexcitation. The three time scales reflect initial inertial dynamics (<20 fs), fast local reorientational and translational motions (a few picoseconds), and slow surface hydration coupled with protein motions (tens of picoseconds).

Similarly, we studied the relaxation dynamics for isomer 2, and the results are shown in Figure 5, where both linear response and nonequilibrium calculations, like isomer 1, exhibit similar dynamics within 140 ps (Figure 5a and b). The parameters extracted by fitting to a sum of exponentials are given in Table 1, including the isomer 1 for comparison. Besides the initial ultrafast components, the indole−protein contribution, in contrast to isomer 1, is dominant during 30−140 ps, and the indole−water contribution in this period is minor. The total Stokes shift calculated for isomer 2 is 22.5 kJ/mol (23.1 kJ/mol from linear response). Closer examination reveals underlying dynamics not apparent in the total Stokes shift or even in the water and protein components. Water molecules within 5 Å from the indole (Figure 5b) exhibit a significant solvation response up to the 140-ps limit of the nonequilibrium simulations in a direction that competes with indole−protein interactions. We also found that the loop backbone makes the major contribution to the indole−protein relaxation.[42] Consistent with the structural flexibility observed in Figure 3, the loop is more mobile. The neighboring charged residues glu4 and lys79 move away from the indole ring (Figure 5d), but their interaction energies with indole also compensate each other (Figure 5c). These results show that the flexible loop backbone dominates overall slow relaxation and both the local protein and the water molecules significantly rearrange, leading to fortuitous cancellations of indole−water contributions in 140 ps.

(68) Young, R. D.; Frauenfelder, H.; Johnson, J. B.; Lamb, D. C.; Nienhaus, G. U.; Philipp, R.; Scholl, R. *Chem. Phys.* **1991**, *158*, 315.

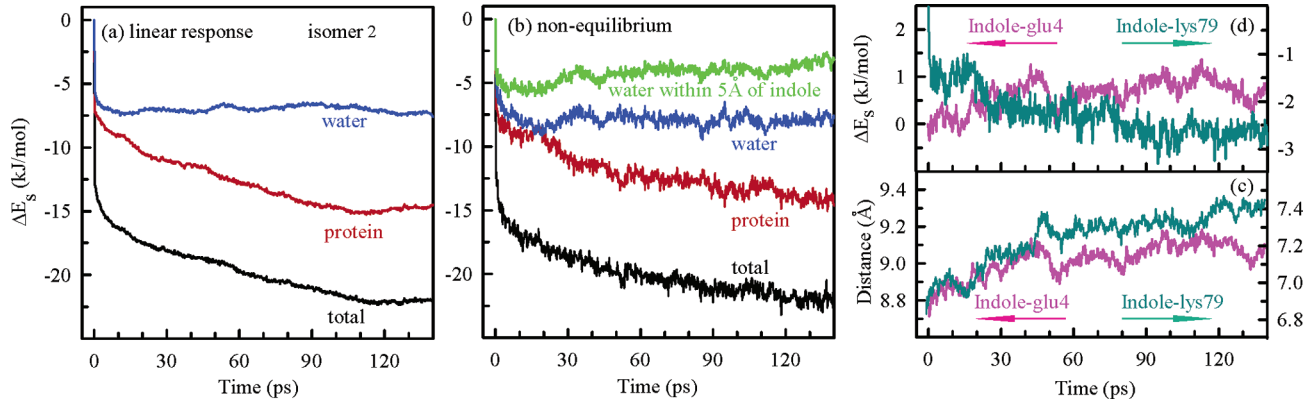

Figure 5. Solvation dynamics from MD simulations for isomer 2. (a) The linear-response calculated time-resolved Stokes shifts for indole−protein, indole−water, and their sum. In contradiction to isomer 1, the indole−protein shows an apparent slow component, but the indole−water exhibits no decay in the simulated time window. (b) Direct nonequilibrium simulations of the time-resolved Stokes shifts for indole−water, indole−protein, and their sum. Similar to (a), the indole−protein relaxation has a slow decay component, and the indole−water lacks apparent decay. Also shown is the indole−water (within 5 Å of indole) with a coupled long-time negative solvation. (c) Relaxation between indole−lys79 and indole−glu4. The interaction energy changes from these two residues nearly cancel each other. (d) The distance changes between the indole and two charged residues, but both residues move away from the indole ring.

Table 1. Total Stokes Shifts Obtained from Linear Response (LR) and Nonequilibrium (NE) MD Simulation for Isomer 1 and Isomer 2[a]

	isomer 1				isomer 2			
	LR		NE		LR		NE	
c_g,τ_g	9.9	0.12	4.0	0.018	12.5	0.13	2.9	0.015
c_{1a},τ_{1a}			6.1	0.080			8.2	0.075
	3.6	1.4			2.7	2.2		
c_{1b},τ_{1b}			4.9	1.6			4.7	1.4
c_2,τ_2	2.0	23	2.7	56	7.9	67	6.7	58
S_∞	−15.5		−17.7		−23.1		−22.5	

[a] Stokes shifts were fitted with $S(t) = c_g e^{-(t/\tau_g)2} + c_1 e^{-(t/\tau_1)} + c_2 e^{-(t/\tau_2)} + S_\infty$, while the nonequilibrium curves required an extra short time exponential, $S(t) = c_g e^{-(t/\tau_g)2} + c_{1a} e^{-(t/\tau_{1a})} + c_{1b} e^{-(t/\tau_{1b})} + c_2 e^{-(t/\tau_2)} + S_\infty$ ($c_g + ... + c_2 + S_\infty = 0$). The amplitudes and time constants are in the units of kJ/mol and ps, respectively. Determining the true parameters of the Gaussian component requires very high time resolution of data points, which was only done for the nonequilibrium simulations.

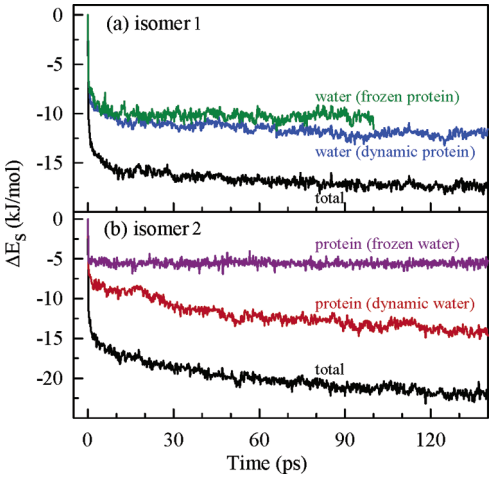

Figure 6. Solvation dynamics from constrained MD simulations. (a) Comparison of indole−water relaxation with and without frozen protein structure for isomer 1. The slow component of the water response nearly disappears, indicating that slow water relaxation needs protein fluctuations. (b) Comparison of indole−protein relaxation with and without frozen water for isomer 2. Similarly, the slow component of the indole−protein disappears, indicating that the protein relaxation also requires water fluctuations.

The simulation results from both isomer 1 and isomer 2 show that the observed solvation dynamics around the Trp7 site can arise from strongly coupled neighboring water and protein relaxation. Judging by the time dependence of their separate contributions to the total response, the Stokes shift over tens of picoseconds can apparently result from either surface water or protein conformational relaxation for isomers 1 and 2, respectively. To elucidate the origin of these observed time scales, we performed frozen protein and frozen water simulations.

Constrained Molecular Dynamics and Origin of Slow Relaxation. MD simulations with either protein or water constrained at the instant of photoexcitation were performed for both isomer 1 and isomer 2. For isomer 1, because surface water relaxation dominates the slow component of the total Stokes shift, in Figure 6a we show the result of simulations of isomer 1 with an ensemble of frozen protein configurations to examine the role of protein fluctuations. Clearly, the long component of indole−water interactions disappears when the protein is constrained. This result shows that without protein fluctuations indole−water relaxation over tens of picoseconds does not occur. Thus, while surface hydrating water molecules seem to drive the global solvation and, from the dynamics of the protein and water contributions, are apparently responsible for the slowest component of the solvation Stokes shift for isomer 1 (Figure 4), local protein fluctuations are still required to facilitate this rearrangement process. When the protein is frozen, the ultrafast contributions (up to a few ps) arise purely from inertial dynamics and surface water reorientations and translations. After these fast relaxation processes are complete, surface water molecules under the rigid protein potential field are still in dynamical equilibrium with outside bulk water on a residence time scale of tens of picoseconds, just as they were when the protein was flexible, but this exchange dynamics does not lead to slow solvation dynamics without protein fluctuations. Protein fluctuations are effectively a part of surface hydration processes.

The fact that the indole−water relaxation is still present under the frozen protein with nearly the same amplitude (Figure 6a) is one indication that the water response is not qualitatively modified by freezing the protein. The rigid potential field of the frozen protein somewhat limits rearrangements of the local water networks, but the difference is quantitative, not qualitative.

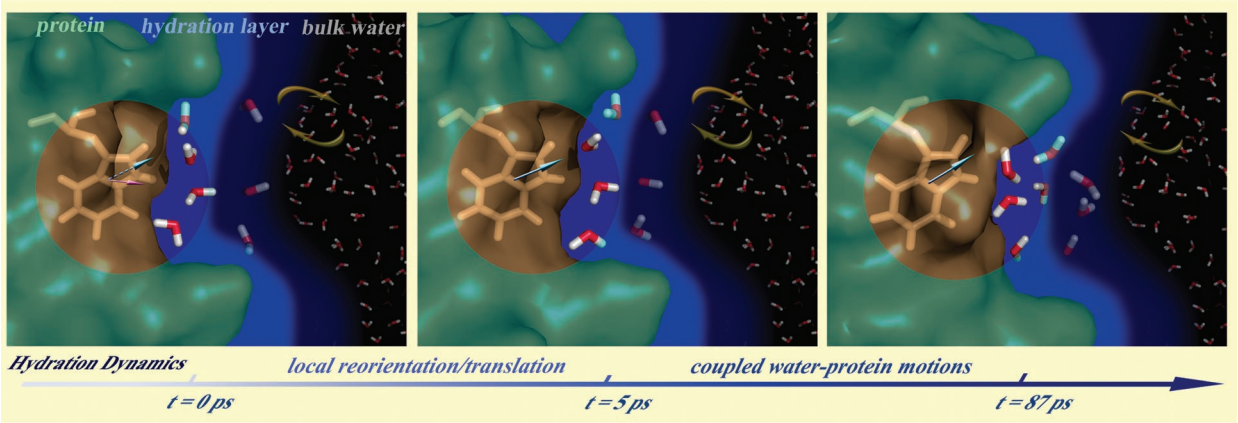

Figure 7. The molecular mechanism of protein surface hydration. Shown here is the Trp7 site with two hydration layers taken from an MD trajectory. Only some water molecules in the layers within 7 Å from the indole ring are shown for clarity. The arrows show a dynamical exchange of hydrating water molecules with bulk water, which occurs at all times. At time zero, the ground-state dipole of the indole is suddenly increased and reoriented by photoexcitation. The neighboring hydrating water molecules rapidly rotate and translate in a few picoseconds. The next stage of the relaxation process is coupled water−protein motions over tens of picoseconds, which gives rise to the slow component of the Stokes shift. During this process, the initial water molecules may also be replaced by outside bulk water.

For isomer 2, protein interactions with the chromophore make the dominant contributions to the slow component of the Stokes shift. Therefore, in Figure 6b, we show simulation results under frozen water conditions. On the subpicosecond time scale, the protein can relax in the constrained water field, but the longer-time indole−protein solvation disappears, indicating that the protein cannot fluctuate under the rigid water potential field. The protein response following photoexcitation also requires water fluctuations. Thus, the slow solvation, protein fluctuations, and the dynamics of hydrating water are all intrinsically related.

Comparison between Simulations and Experiments. Experiments and MD simulations both found biphasic relaxation dynamics occurring on similar time scales, a few and tens of picoseconds, and with similar magnitude. The simulations enable a molecular interpretation of the slow component seen in experiments. However, some serious discrepancies currently exist: (1) The total Stokes shifts from nonequilibrium calculations, 17.7 kJ/mol for isomer 1 and 22.5 kJ/mol for isomer 2, are significantly larger than the experimental result, 7.9 kJ/mol, and (2) no ultrafast decay (or inertial motion) in less than 1 ps in the experiments was observed, but the simulations gave more than 50% of the total energy on this time scale for both isomers. These discrepancies would be resolved if the large inertial response seen in simulations were removed, either by improvement of the force field, such as by incorporation of electronic polarization,[69,70] or by inclusion of electronically non-adiabatic effects that might suppress the inertial regime. Further work is required to achieve quantitative agreement between theory and experiment. At this point, our use of standard force fields allows us to explain the origin of the Stokes shift after ∼1 ps, and to compare with and reinterpret previous theoretical studies.

Conclusions

With femtosecond temporal and single-residue spatial resolution, we experimentally observed solvation dynamics at a particular site (Trp7) of apomyoglobin, yielding a biphasic distribution in a few and tens of picoseconds. From the linear-response and direct nonequilibrium molecular dynamics calculations on myoglobin, we observed a similar biphasic distribution, as well as a pronounced inertial decay not observed in experiments. Neither our experiments nor theory probed dynamics on time scales longer than several hundred picoseconds.

The molecular mechanism underlying slow relaxation processes near hydrated proteins, such as the long component in the observed fluorescence Stokes shift, has been analyzed by several groups. Bagchi, Zewail, and co-workers[19,71] proposed that the observed slow dynamics near proteins is an inherent feature of water in the potential field of a protein and is directly related to the water residence times at the sites. They emphasize the importance of the dynamic exchange between bound water near the protein and "quasi-free" water in the hydration layer. In contrast, Nilsson and Halle[28] recently argued that water−protein interactions are comparable to water−water interactions. They concluded that the local dynamics of water close to protein, while not identical to bulk water, should not be on a vastly different time scale. In a simulation of the protein monellin, they attributed the reported slow relaxation to protein motion because they observed a slow component in the protein contribution to the Stokes shift, but not in the water contribution.

We have found that longer-time solvation over tens of picoseconds near Trp7 in myoglobin results from strongly coupled water−protein motions. By freezing either protein or water in either isomer 1 or 2, the long component disappears. Thus, the tens of picoseconds we observed in relaxation represent the time scale of local water−protein fluctuations. Both the Bagchi−Zewail[19,71] and the Nilsson−Halle[28] models have elements that are applicable to the case of Trp7 in myoglobin. The former revealed the possible relationship between the observed solvation time with water residence time and emphasized the role of water fluctuations, but not in the context of coupled water−protein fluctuations observed here for myoglobin. The latter emphasized the role of protein fluctuations, but for the wrong reason, a slow time component seen in the protein contribution to the total Stokes shift. Our results show even when a slow component in the protein contribution to the Stokes shift is not evident, as is true for isomer 1, protein (and water)

(69) Bader, J. S.; Berne, B. J. *J. Chem. Phys.* **1996**, *104*, 1293.
(70) Kumar, P. V.; Maroncelli, M. *J. Chem. Phys.* **1995**, *103*, 3038.
(71) Bhattacharyya, S. M.; Wang, Z. G.; Zewail, A. H. *J. Phys. Chem. B* **2003**, *107*, 13218.

flexibility is still required to observe the slow component in the total Stokes shift.

The molecular mechanism of biphasic relaxation is shown in Figure 7 upon excitation of Trp7. The first 5 ps is dominated by local motions, like reorientation and translation of hydrating water molecules. While water motions in the hydration layer are significantly longer than bulk water, water dynamics alone does not give rise to slow components in the Stokes shift that extend over tens of picoseconds. Instead, strongly coupled water−protein fluctuations are required. Constraining either the protein or the water eliminates the slow component (Figure 6). The interactions of surface water with protein fluctuations are an integral part of hydration dynamics, particularly at longer times. For the first time, we determined the actual time scale of coupled water−protein fluctuations around the site of Trp7 (∼90 ps) from both an experimental and a theoretical point of view. The dynamics of water−protein fluctuations is biologically significant and relevant, and it is shown now to occur on tens of picoseconds.

Acknowledgment. We thank Prof. Stephen Sligar (UIUC) for generously providing us the myoglobin plasmid (pMb122), and Prof. Ahmed H. Zewail (Caltech) for many stimulating discussions and constructive comments. Also, we thank Lijuan Wang, Luyuan Zhang, and Weihong Qiu for the initial help with the experiments. This work was supported in part by the Packard Foundation Fellowship and the National Science Foundation to D.Z. (CH-0517334).

Supporting Information Available: Complete ref 66. This material is available free of charge via the Internet at http://pubs.acs.org.

JA0685957